

Classification of EEG signals using normal inverse Gaussian parameters in the dual-tree complex wavelet transform domain for seizure detection

Anindya Bijoy Das · Mohammed Imamul Hassan Bhuiyan · S. M. Shafiqul Alam

Received: 12 September 2014 / Revised: 1 December 2014 / Accepted: 7 December 2014 / Published online: 31 December 2014
© Springer-Verlag London 2014

Abstract In this paper, a comprehensive method using symmetric normal inverse Gaussian (NIG) parameters of the sub-bands of EEG signals calculated in the dual-tree complex wavelet transformation domain is proposed for classifying EEG data. The suitability of the NIG probability distribution function is illustrated using statistical measures. A support vector machine is employed as the classifier of the EEG signals, wherein the NIG parameters are used as features. The performance of the proposed method is studied using a publicly available benchmark EEG database for various classification cases that include healthy, inter-ictal (seizure-free interval) and ictal (seizure), non-seizure and seizure, healthy and seizure, and inter-ictal and ictal, and compared with that of several recent methods. It is shown that in almost all the cases, the proposed method can provide 100 % accuracy with 100 % sensitivity and 100 % specificity while being faster as compared to the time–frequency analysis-based and EMD techniques.

Keywords Electroencephalogram (EEG) · Seizure · Dual-tree complex wavelet transform (DT-CWT) · Normal inverse Gaussian (NIG) · Support vector machine (SVM)

A. B. Das (✉) · M. I. H. Bhuiyan
Department of Electrical and Electronic Engineering,
Bangladesh University of Engineering and Technology, Dhaka,
Bangladesh
e-mail: anindya149@yahoo.com

M. I. H. Bhuiyan
e-mail: imamhas@gmail.com

S. M. S. Alam
Department of Electrical and Computer Engineering,
Kansas State University, Manhattan, KS, USA
e-mail: sm.salam02@gmail.com

1 Introduction

Among the various neurological disorders, epilepsy is perhaps the most important, considering its prevalence among a large population of the world. Epilepsy is characterized by unprovoked recurring seizures that arises out of excessive and hyper-synchronous activities of neurons in the brain. Seizure may be accompanied by the loss of consciousness/convulsions, decline in cognitive ability and may lead to injury, sometimes to death. Electroencephalogram (EEG) signals represent electrical activities in the neurons of the brain and are obtained from electrodes inserted intracranially or on the scalp. EEG signals are widely used as convenient and relatively inexpensive means for epilepsy diagnosis and management [1]. Highly trained neurologists monitor long-term EEG signals for seizure detection, and epilepsy diagnosis, in general. However, this is a tedious, time-consuming and expensive task. An automated method of seizure detection can assist the neurologist since he will then have to monitor the sections of EEG records around the detected portion only. In addition, automated seizure detection may be used for implantable and closed-loop neuro-stimulation devices for seizure suppression such as the responsive neurostimulators (RNS) [2], as well as to localize the epileptogenic regions of the brain in order to avoid any undue morbidity and ensure effective epilepsy surgery.

Various algorithms have been proposed in the literature for automatic detection of seizures [3–20]. The indispensable part of a detection algorithm is the extraction of the appropriate features to discriminate the EEG signals. The detection process is carried out by extracting the features from an EEG signal and classify them into the appropriate categories such as seizure (ictal) and non-seizure (non-ictal). A widely used approach to process nonlinear signals such as the EEG is to decompose them into time–frequency sub-bands and subse-

quently perform the process using features extracted from the sub-bands [3, 21]. Among various methods, those using features obtained in time–frequency domains have been shown to be highly promising in the detection of seizures. One of the reasons for this is that the diverse processes of brain dynamics and associated neuronal activities are more properly represented in time–frequency sub-bands as compared to the original EEG [6]. Another reason may be that the seizure events often evolve as increased spike or poly-spike-like activities that are expected to be better visualized in the time–frequency domain. Recently, the dual-tree complex wavelet transform (DT-CWT) has been introduced by Selesnick and Kingsbury et al. [22] as a better time–frequency representation of signals as compared to the traditionally used discrete wavelet transform (DWT), widely used in the EEG literature for their analysis of epileptiform activities. The DT-CWT has also been extensively used for the processing of images and video signals [18–30]. However, research reports on the use of DT-CWT for the processing of biological signals, especially EEG signals is rather limited [18, 19, 29]. In [18], ANN- and SVM-based classifiers are proposed using the variance of the DT-CWT sub-bands as features. While the variance represents a statistical average of a signal, the underlying statistics of a signal is more properly described by using an appropriate prior. It is relevant to mention that, in general, utilizing the statistics of the DT-CWT coefficients of image and video signals employing suitable priors has been shown to provide an improved performance in the processing of these signals [23–27]. Thus, it would be interesting to develop classifiers for discriminating EEG signals using the parameters of a prior that can suitably describe the statistics of these signals in DT-CWT domain. The objective of this paper is to develop SVM-based classifiers for the diagnosis of epilepsy and detection of seizure using the parameters of a symmetric normal inverse Gaussian prior extracted from DT-CWT sub-bands as features. Initial results of the present paper about the ability of the NIG parameters in discriminating the EEG signals are presented in [19]; it is shown that on average, the values of the NIG parameters for healthy, inter-ictal and ictal EEG segments are quite distinguishable. It should be mentioned that no classification of EEG signals is carried out in [19]. In the present paper, the appropriateness of the NIG prior in modeling the DT-CWT coefficients of various types of EEG signals is demonstrated, and the distinguishable nature of the NIG parameters is illustrated. The effectiveness of the proposed method is comprehensively studied using a publicly available EEG database for a number of clinically relevant classification cases and compared to those of the state-of-the-art techniques.

In this study, in summary, the NIG parameters calculated from the DT-CWT sub-bands of EEG signals are used to develop SVM-based classifiers. The ability of these classifiers in discriminating EEG signals into several clinically

relevant cases is investigated. The performance is measured in terms of accuracy, sensitivity, specificity, and compared with that of several recent methods.

2 Methodology

In this section, the modeling of the EEG signals in DT-CWT domain using an NIG probability density function (pdf) and the ability of the NIG parameters calculated from the DT-CWT coefficients of these signals in discriminating them is briefly discussed.

2.1 The EEG database

The EEG signals are obtained from a widely used database, publicly available in the Web site of Bonn University [31, 32]. The database consists of 500 single-channel EEG segments of 23.6-s duration each. There are five sets of grouped data, namely A, B, C, D, and E each containing 100 EEG segments. Sets A and B consist of surface EEG segments collected from five healthy volunteers, using the international standard 10–20 electrode placement scheme, in awake and relaxed state, with their eyes open and closed, respectively. Recordings in Sets C and D are obtained from the electrodes placed hippocampal formation of the opposite hemisphere and in the epileptogenic zone, respectively. Data in Set E are collected intra-cranially from these electrodes as well as those implanted in temporal and basal regions of the neocortex. The EEG data in Sets C and D correspond to seizure-free epochs, whereas the recordings in Set E correspond to seizure attacks. All the EEG signals are recorded using the same 128-channel amplifier system and digitized at 173.61 Hz with a 12-bit resolution. Thus, the sample length of each segment is $173.61 \times 23.6 \approx 4,097$, and the corresponding bandwidth is 86.8 Hz. However, the frequency range of an EEG signal usually spans over 0–60 Hz. The frequencies greater than 60 Hz may be considered as noise [6]. On the other hand, the highest frequency component of an EEG segment of the database is 86.8 Hz since the sampling frequency is 173.61 Hz. The frequencies beyond 60 Hz are thus removed by using a sixth-order Butterworth filter.

2.2 Dual-tree complex wavelet transform (DT-CWT)

It is reported in the literature that the DWT is useful for feature extraction in time–frequency domain and analysis of EEG signals to detect epileptiform activities [4, 6, 10]. This is mainly due to its ability to provide an efficient sparse representation of non-stationary signals through time–frequency localization. However, the DWT has a number of drawbacks that include oscillatory nature of wavelets (limiting its performance around singularities), lack of shift invariance, aliasing, and limited directional information [22]. The DT-

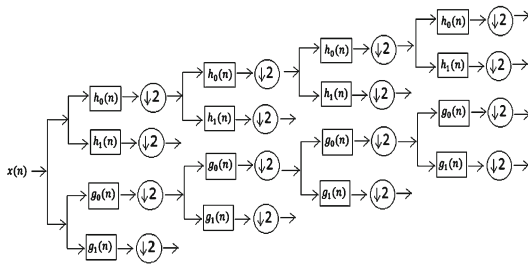


Fig. 1 1D dual-tree complex wavelet transformation

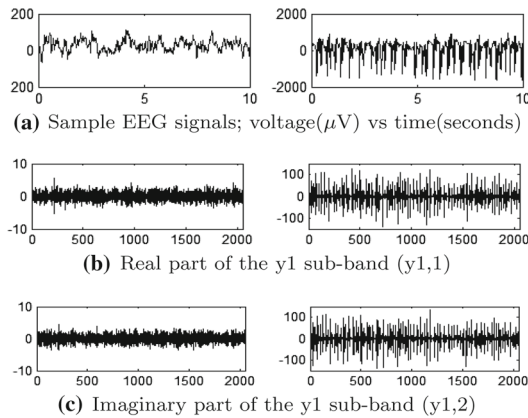


Fig. 2 Sample EEG signals from Sets D and E and the corresponding DT-CWT coefficients; plots on the *left column* correspond to the sample EEG signals from Set D and its DT-CWT sub-bands, whereas those in the *right column* to that of Set E

CWT offers a better time–frequency representation of non-stationary signals by ameliorating these problems of DWT through the implementation of a discrete complex wavelet transform using separable filter banks as in the DWT. Basically, it employs two real DWT trees, where the tree on the top (See Fig. 1) represents the real part of the complex wavelet coefficient, whereas the bottom one the imaginary part. The DT-CWT coefficients are non-oscillating with a nearly shift-invariant magnitude and significantly reduced aliasing with more directionalities as compared to the DWT and UDWT, while being only 2^d times redundant for signals with dimension d . The non-oscillating magnitude and low computational complexity (due to a modest redundancy) make the DT-CWT a better and attractive choice for the analysis of nonlinear signals such as EEG. Figure 2 shows the plots of sample EEG segments of 10s from the datasets D (top left) and E (top right) in the first row. The plots of the corresponding first level DT-CWT real and imaginary coefficients are shown in the second and third rows, respectively.

In this paper, the parameters of an NIG pdf are estimated from the various sub-bands of a four-level DT-CWT decomposition of the filtered EEG signals. After the first level of decomposition, the EEG signal, X (0–60 Hz), is decomposed into its higher resolution components $y1$ (30–60 Hz) and lower resolution components, $z1$ (0–30 Hz). In the sec-

ond level, the $z1$ component is then decomposed into higher resolution components, $y2$ (15–30 Hz) and lower resolution components, $z2$ (0–15 Hz). Thus, the components obtained after four levels of decomposition include the sub-bands $z4$ (0–4 Hz), $y4$ (4–8 Hz), $y3$ (8–15 Hz), $y2$ (15–30 Hz), and $y1$ (30–60 Hz). Reconstructions of these five components using the inverse DT-CWT approximately correspond to the five physiological EEG sub-bands delta, theta, alpha, beta, and gamma, respectively [6]. Although, the sub-bands might overlap, it is insignificant considering their physiologically approximate nature. Since, each DT-CWT coefficient has two parts, real and imaginary, the four-level decomposition yields ten sub-bands in total (five for real and five for imaginary). In the present paper, the real and imaginary parts of the DT-CWT sub-bands are represented by $(y1,1)$, $(y1,2)$, $(y2,1)$, $(y2,2)$, $(y3,1)$, $(y3,2)$, $(y4,1)$, $(y4,2)$, $(z4,1)$, and $(z4,2)$. For example, $(y1,1)$ and $(y1,2)$ represent the real and imaginary parts of the $y1$ sub-band.

2.3 Modeling of the EEG signals using an NIG pdf

It is assumed that the symmetric NIG pdf can appropriately model the statistics of EEG signals in DT-CWT domain. The motivation for using the NIG pdf arises from its success in modeling the statistics of nonlinear signals with heavy-tailed statistics, for example, financial data, hydrophone data, economics data, images, and video signals, among others [24–26, 33–36]. The symmetric NIG pdf is a variance mean mixture density where the inverse Gaussian density is the mixing distribution and expressed as

$$P_{\alpha, \delta}(x) = \frac{A(\delta, \alpha) K_1(\alpha \sqrt{\delta^2 + x^2})}{\sqrt{(\delta^2 + x^2)}} \tag{1}$$

where K_1 is the first-order modified Bessel function of the second kind, $A(\delta, \alpha) = \frac{\delta \alpha}{\pi} \exp(\delta \alpha)$, and X represents the DT-CWT coefficients of an EEG signal. The steepness of the pdf is controlled by α in that, as it is increased, it becomes steeper. The other parameter δ is a scale factor that controls its dispersion. Figure 3 shows the plots of the pdf for various values of α and δ . Figure 4 shows the empirical pdfs of DT-CWT sub-band $(y1,1)$ of EEG recordings from Sets A, C, and E. It is seen that the pdfs are of different shapes in terms of peakedness and dispersion and demonstrate heavy-tailedness, especially for Set E. Figure 5 provides the variance stabilized $p - p$ plots of the empirical pdfs (shown in Fig. 4), and the NIG and zero-mean Gaussian pdfs used to model the corresponding EEG sub-bands. The $p - p$ plot is obtained by plotting $F_a(x)^t$ against $F_e(x)^t$ where

$$F_a(x)^t = \frac{2}{\pi} \arcsin \left\{ \sqrt{F_a(x)} \right\} \tag{2}$$

$$F_e(x)^t = \frac{2}{\pi} \arcsin \left\{ \sqrt{F_e(x)} \right\} \tag{3}$$

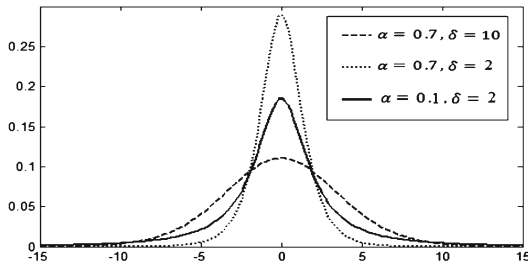


Fig. 3 Plots of NIG pdf for various values of α and δ

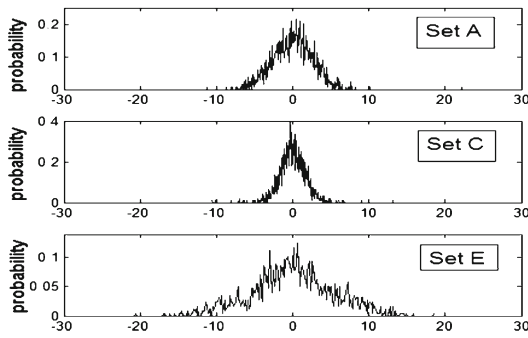


Fig. 4 Plots of the empirical pdfs for real part of the sub-band $y_1(y_{1,1})$ of three samples of EEG signals from the Sets A, C, and E

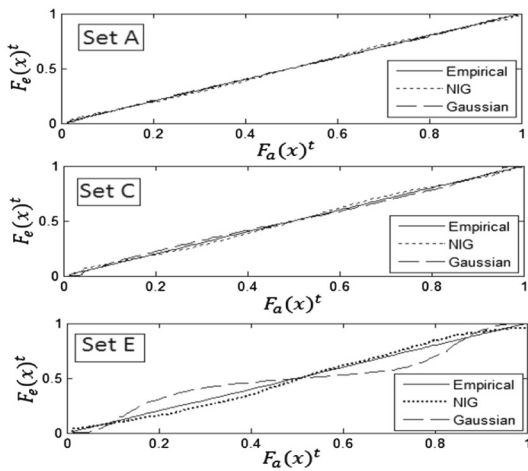


Fig. 5 $p - p$ plots of the empirical, NIG, and Gaussian pdfs for the real parts of sub-band $y_1(y_{1,1})$ for three sample EEG signals

$F_a(x)$ and $F_e(x)$ denote the cumulative density function(cdf) of a prior pdf and the empirical cdf, respectively [33]. In order to obtain the plots, the NIG parameters are estimated from the corresponding DT-CWT sub-bands as [25]

$$\alpha = \sqrt{\frac{3K_x^2}{K_x^4}} \tag{4}$$

$$\delta = \alpha K_x^2 \tag{5}$$

where The second- and fourth-order cumulants of an NIG pdf are denoted as K_x^2 and K_x^4 , respectively.

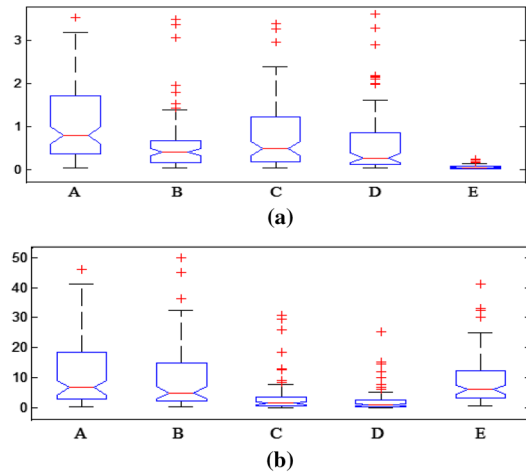


Fig. 6 Box plots of **a** α and **b** δ for $(y_1,1)$

From Fig. 5, it is seen that for Set A and Set C, the NIG and Gaussian pdfs provide a close fit to the empirical ones. However, for Set E, the NIG pdf provides a superior fit as compared to that of the Gaussian pdf. Note that an NIG pdf tends to a Gaussian one with variance $\frac{\delta}{\alpha}$ as $\alpha \rightarrow \infty$ [33]. Thus, the Gaussian pdf is a special case of the NIG pdf. Considering this fact and our observations from the $p - p$ plots, the NIG pdf is more appropriate for modeling various types of EEG data in DT-CWT domain as compared to a Gaussian pdf.

Finally, in Fig. 6, the box plots are shown for the five sets using the values of α and δ , respectively, estimated from the real parts of the y_1 sub-bands that is $(y_1,1)$. From the box plots, it is clear that the NIG parameters can discriminate the EEG data quite well. Overall, the discussion in this section indicates that (i) an NIG pdf is a highly suitable prior for modeling the statistics of EEG signals in the DT-CWT domain and (ii) the NIG parameters can distinguish EEG signals effectively. Based on these observations and the results of [19] about the discriminating ability of the NIG parameters, support vector machine (SVM)-based classifiers are developed in the next section where the NIG parameters are utilized as features.

3 Proposed SVM-based classification of EEG signals

3.1 Support vector machine (SVM)

A support vector machine (SVM) is a binary classifier, which projects the nonlinear but separable data onto a higher dimensional space by using an appropriate kernel function and subsequently determining the best hyperplane to separate the data in the projected space. One of the advantages of using an SVM is its automatic complexity control to avoid overfitting [37]. The reason for choosing the SVM is its wide use

in pattern classification, regression, and density estimation. A proper kernel function for a certain problem is dependent on the specific data. In this paper, radial-basis function (RBF) kernel is used as it yields a better performance as compared to the other kernel functions. Although the SVM is a binary classifier, it may be used to solve multi-class problems by combining several of its kind. In this paper, the error-correcting output coding (ECOC) approach obtained from digital communication [38] is employed for that purpose. A maximum of $2^{n-1} - 1$ SVMs are trained for separating n classes. For example, to separate three classes (X, Y, and Z), three classifiers are used: the first SVM classifies X from Y and Z, the second Y from X and Z, and the third Z from X and Y. The classifier-output code for a pattern is a combination of targets of all the separate SVMs. In the previous example, vectors from classes X, Y, and Z have codes (1,−1,−1), (−1,1,−1), and (−1,−1,1), respectively. If each of the separate SVMs classifies a pattern correctly, the classifier-target code is met and the ECOC approach reports no error for that pattern. Notice that for the binary (two way) classification purposes, a single SVM is sufficient.

3.2 The proposed classification method

For the SVM-based classification, first the features of classification are extracted. Due to the non-stationary nature of the EEG data, prior to feature extraction, an EEG record is first divided into 16 non-overlapping segments where each of the segments is assumed to be stationary. As there are 100 EEG datasets from each of the Sets A, B, C, D, and E, in total, $500 \times 16 = 8,000$ segments are generated. Next, each of the segments is subjected to a four-level DT-CWT decomposition, giving 10 sub-bands for each. Subsequently, the NIG parameters α and δ are estimated from each sub-band using (6) and (7). For example, Set A has $100 \times 16 = 1,600$ segments and $1,600 \times 10 = 16,000$ sub-bands, thus 16,000 values of α and δ each are obtained for Set A. Next, training and testing are carried out using the extracted features. For a particular set, half of the segments, chosen randomly, are used for training and the rest half for testing in an SVM classifier. For example, if the target is to discriminate the segments of Set A from those of Set E, then among the 1,600 segments of Set A, 800 segments are used for training and the rest 800 for testing. The distribution is same for the Set E.

4 Results of the experiments

In this Section, the performances of the proposed SVM-based classifiers are described and compared to those of the state-of-the-art methods using well-known figures of merit, sensitivity (sen), specificity (spec), and accuracy (acc) [5] for various classification cases. For the five sets of EEG records

Table 1 Classes considered for classification

Cases	Sets	Description
I	(A, B), (C, D) and E	Healthy, inter-ictal and ictal
II	(A, B, C, D) and E	Non-seizure and seizure
III	A and E	Healthy and seizure
IV	A, D and E	Healthy, inter-ictal and ictal
V	D and E	Inter-ictal and ictal
VI	C and E	Inter-ictal and ictal

described earlier, six different cases of classification are considered. The cases are chosen based on their clinical relevance and use in various papers in the literature to facilitate comparison and shown in Table 1.

Here, the healthy class includes the signals acquired from healthy people, whereas the inter-ictal class includes the seizure-free epochs of the epilepsy patients, and ictal class includes the seizure epochs. As for clinical relevance, Cases I and IV are related to the discrimination of healthy persons from the epilepsy patients as well as occurrence of seizures. It may also be relevant to the fact that in some cases, inter-ictal epileptiform discharges are observed for healthy persons, whereas about 10% epilepsy patients never show such discharges. Cases II and III correspond to the detection of seizure and, in addition, may be related to the discrimination of surface EEGs from the intra-cranial ones since Sets A, B and C, D, E are acquired from surface and intra-cranial electrodes, respectively. Case V corresponds to the detection of the onset of seizure, since the signals in Set D are obtained from epileptogenic zone and thus highly related to the early-ictal activities. Similarly, Case VI is related to discriminating the ictal recordings from the inter-ictal ones. Overall, the cases are relevant to epilepsy diagnosis and seizure detection.

The performance of the proposed method is first studied using the features from a DT-CWT sub-band. Table 2 shows the corresponding values of sensitivity, specificity, and accuracy obtained by using the features from various sub-bands. It is seen that features obtained from the high-frequency sub-bands, such as y1, y2 or y3 sub-bands, provide better performances than those of the low-frequency ones, for example y4 and z4. Next, the performance is studied for various cases using different combinations of features obtained from y1, y2, and y3 sub-bands. The corresponding values of the sensitivity (sen), specificity (spec), and accuracy (acc) are provided in Table 3. It is seen that the performance of the proposed method improves significantly when features from two or more sub-bands are used. The best performance is achieved when features from the three sub-bands y1, y2, and y3 are used, in conjunction, giving 100% accuracy with 100% sensitivity and 100% specificity with the exception of Case I. However, in Case I, the accuracy is quite high, about

Table 2 Classification performance for features from single-level sub-bands

Cases	Per	Names of the used feature vectors				
		y1	y2	y3	y4	z4
Case I (AB), (CD), and E	Sen (AB)	86.34	93.84	84.38	87.28	83.59
	Sen (CD)	82.59	89.59	91.75	77.88	77.34
	Sen (E)	96.75	97.69	97.69	95.31	94.38
	Acc	86.925	92.91	90.54	85.13	81.65
Case II ABCD and E	Sen	97.13	98.06	97.75	94.13	92.5
	Spec	94.41	95.52	96.19	92.22	88.3
	Acc	94.95	96.03	96.5	92.6	89.13
Case III A, E	Sen	97.5	98.63	99.38	97.13	94.94
	Spec	94	98.75	98.5	94.88	93.94
	Acc	95.75	98.69	98.94	96	94.44
Case IV A, D, E	Sen (A)	83.25	93.19	95.5	88.69	85.38
	Sen (D)	91.19	95.94	97.38	92.94	87.62
	Sen (E)	95.69	97.94	99	96.75	92.75
	Acc	90.04	95.69	97.29	92.79	88.58
Case V D, E	Sen	95.38	98.25	98.25	95.31	93.88
	Spec	96.63	97.5	95.63	94.88	92.44
	Acc	96	97.88	96.94	95.09	93.16
Case VI C, E	Sen	97.88	98.25	98.93	94.63	92.38
	Spec	95.44	96.88	97.36	95.81	94.13
	Acc	96.66	97.56	98.14	95.22	93.25

96%. Due to the mis-classification of classes A and B, and the classes C and D, into the class E, 100% accuracy is not achieved. It is also seen that 100% sensitivity is achieved for Set E which indicates that the signals in Set E are accurately discriminated from the signals in Sets A, B, C, and D. Thus, the clinical effect of this classification error is much less as compared to a mis-classification of the signals in Set E. It is also observed that the sensitivity for Classes (A, B) and (C, D) are 95.84 and 94.84%, respectively, which indicates that a very small number of segments are mis-classified for these classes. Note that the signals in Sets A and B are obtained from healthy persons, whereas those in Set C and D are collected during inter-ictal periods, thus the neurologists can discard the related false alarms.

The performance of the proposed method is compared with that of several state-of-the-art algorithms in Table 4. For Case I, the proposed method gives an accuracy, significantly higher than that of [5], and also higher than that of in [17], and almost the same as that of [7]. However, the number of features used for [7] is 40, whereas for the proposed method, it is 12 only. For the other cases, the proposed method provides 100% accuracy with 100% sensitivity and 100% specificity. Note that the method of [18] uses variance, calculated as sample variance, as features in an SVM for classifying EEG signals. The sample variance is the maximum likelihood

Table 3 Classification performance for features from multi-level sub-bands

Cases	Results	Names of the used feature vectors			
		y1, y2	y1, y3	y2, y3	y1, y2, y3
Case I (AB), (CD) and E	Sen (AB)	94.25	92.84	95.16	95.84
	Sen (CD)	93.91	92.38	93.09	94.84
	Sen (E)	98.69	98.5	99.88	100
	Acc	95	93.79	95.28	96.28
Case II ABCD, E	Sen	99	98.75	99.94	100
	Spec	99.36	99.47	99.81	100
	Acc	99.29	99.33	99.83	100
Case III A, E	Sen	99.76	99.63	100	100
	Spec	99.63	99.76	99.88	100
	Acc	99.69	99.69	99.94	100
Case IV A, D, E	Sen (A)	95.56	98.13	99	100
	Sen (D)	97.38	98.38	99.06	100
	Sen (E)	98.94	99.25	99.56	100
	Acc	97.29	98.58	99.21	100
Case V D, E	Sen	99.88	99.63	99.5	100
	Spec	99.88	99.38	100	100
	Acc	99.88	99.5	99.75	100
Case VI C, E	Sen	99.06	100	99.88	100
	Spec	98.44	99.94	98.94	100
	Acc	98.75	99.97	99.41	100

(ML) estimate of a zero-mean Gaussian pdf. In this respect, the results of [18] can be regarded as that obtained from an SVM classifier using Gaussian parameters. It is noted from Table 4 that for classification schemes other than binary (two way) ones, the use of NIG parameters, as compared to that of employing Gaussian parameters, yields better accuracy.

The proposed method is also computationally fast. It is implemented in MATLAB [39] on a desktop computer with an Intel core to duo 2.66 GHz processor and 2 GB RAM. The time required to extract the necessary 12 features from a segment of 23.6/16 \approx 1.475 s, is 0.003–0.005 s. In [7, 9], time-frequency features are extracted from a recording of 23.6 s and the feature extraction time varies from 3.8–4.09 s. In [5], features are extracted from a recording of 1.475 s, but the feature extraction time is 0.2–0.6 s. For testing, the SVM-based classifiers require typically 0.05 and 0.02 s, respectively, for Cases I, IV and Cases II, III, V, VI (to identify the appropriate class of an EEG segment). Thus, for example, for a 24-h continuous EEG recordings of epilepsy patients (consisting Sets D and E type segments), the processing time of the proposed method for seizure detection can be expected to be around 24 min. The computational performance can be further improved by developing a standalone C/C++ program for the proposed method and implementing it on multiple cores in parallel fashion.

Table 4 Comparison of classification performance obtained for various algorithms

Cases	Methods	Acc (%)
I (AB), (CD) and E	Tzallas et al. [7]	97.72
	Orhan et al. [17]	95.6
	Alam et al. [5]	80
	Das et al. [18]	83.5
	Proposed	96.28
II (ABCD), E	Tzallas et al. [7]	97.73
	Kumar et al. [10]	94
	Orhan et al. [17]	99.6
	Liang et al. [12]	98.51
	Alam et al. [5]	100
	Chen et al. [20]	100
	Das et al. [18]	100
	Proposed	100
III A, E	Tzallas et al. [9]	100
	Bedeuzzaman et al. [13]	97.75
	Nicolaouet al. [15]	93.55
	Orhan et al. [17]	100
	Kumar et al. [10]	100
	Alam et al. [5]	100
	Chen et al. [20]	100
	Das et al. [18]	100
	Proposed	100
IV A, D, E	Tzallas et al. [7]	99.28
	Tzallas et al. [9]	100
	Liang et al. [12]	98.67
	Orhan et al. [17]	96.67
	Alam et al. [5]	100
	Das et al. [18]	96.8
	Proposed	100
IV D, E	Liang et al. [12]	98.74
	Nicolaouet al. [15]	79.94
	Kumar et al. [10]	95
	Alam et al. [5]	100
	Das et al. [18]	100
VI C, E	Proposed	100
	Nicolaouet al. [15]	88
	Kumar et al. [10]	100

5 Conclusion

In this paper, a SVM-based method has been proposed using statistical NIG parameters computed in DT-CWT domain as features for the automatic seizure detection and epilepsy. The suitability of an NIG pdf in modeling EEG signals in DT-CWT domain has been demonstrated. The discrimination of EEG signals using the NIG parameters in the DT-CWT

sub-bands has been discussed. SVM classifiers have been developed for binary as well as multi-way classification, the latter employing the ECOC approach. The performance of the SVM-based classification has been studied for a number of clinically relevant cases. It has been shown that the parameters obtained from the three high-frequency DT-CWT sub-bands yield 100 % sensitivity, specificity, and accuracy. Furthermore, the proposed method gives 100 % accuracy in all the cases except one for which the accuracy is also quite high, about 96 %. However, the corresponding sensitivity for ictal classes has been found to be 100 % indicating accurate detection of actual seizure events. In comparison with several state-of-the-art algorithms, the proposed method has been shown to provide better or at least almost the same accuracy in detecting seizure and epilepsy. The proposed method has also been shown to be computationally fast in terms of feature extraction and seizure detection. The overall performance and computational speed suggest that it can be useful for automated analysis/monitoring of clinically used continuous EEG records. Since the proposed method uses the statistics of EEG signals in time–frequency domain, similar performance is expected by the proposed classifiers for the long-term EEG records. Currently, the authors of the present paper are conducting a study using long-term EEG records.

References

1. Smith, S.J.M.: EEG in the diagnosis, classification, and management of patients with epilepsy. *J. Neurol. Neurosurg. Psychiatry*, **76** (Suppl II), ii2–ii7 (2005)
2. Salam, M.T., Sawan, M., Nguyen, D.K.: Low-power implantable device for onset detection and subsequent treatment of epileptic seizures. *J. Healthc. Eng.* **1**(5), 169–184 (2010)
3. Bajaj, V., Pachori, R.B.: Classification of seizure and nonseizure EEG signals using empirical mode decomposition. *IEEE Trans. Inf. Technol. Biomed.* **16**, 1135–1142 (2012)
4. Liu, Y., Zhou, W., Yuan, Q., Chen, S.: Automatic seizure detection using wavelet transformation and SVM in long term intracranial EEG. *IEEE Trans. Neural Syst. Rehabil. Eng.* **20**(6), 749–755 (2012)
5. Shafiul Alam, S.M., Bhuiyan, M.I.H.: Detection of seizure and epilepsy using higherorder statistics in the EMD domain. *IEEE J. Biomed. Health Inform.* **17**(2), 312–318 (2013)
6. Adeli, H., Ghosh-Dastidar, S., Dadmehr, N.: A wavelet-chaos methodology for analysis of EEGs and EEG sub-bands to detect seizure and epilepsy. *IEEE Trans. Biomed. Eng.* **54**(2), 205–211 (2007)
7. Tzallas, A.T., Tsipouras, M.G., Fotiadis, D.I.: Automatic seizure detection based on time-frequency analysis and artificial neural networks. *Comput. Intell. Neurosci.* **11**(03), 288–295 (2007). Hindawi Publishing Corporation
8. Srinivasan, V., Eswaran, C., Sriraam, N.: Approximate entropy-based epileptic EEG detection using artificial neural networks. *IEEE Trans. Inf. Technol. Biomed.* **11**(3), 288–295 (2007)
9. Tzallas, A.T., Tsipouras, M.G., Fotiadis, D.I.: Epileptic seizure detection in EEGs using time-frequency analysis. *IEEE Trans. Inf. Technol. Biomed.* **13**(5), 703–710 (2009)

10. Kumar, Y., Dewal, M.L., Anand, R.S.: Epileptic seizures detection in EEG using DWT-based ApEn and artificial neural network. *Signal Image Video Process.* **8**(7), 1323–1334 (2012)
11. Subasi, A., Gursoy, M.I.: Classification of electroencephalogram signals with combined time and frequency features. *Expert Syst. Appl.* **38**(8), 10499–10505 (2011)
12. Liang, S.F., Wang, H.C., Chang, W.L.: Combination of EEG complexity and spectral analysis for epilepsy diagnosis and seizure detection. *EURASIP J. Adv. Signal Process.* **2010**, article id. 853434, Hindawi Publishing Corporation (2010)
13. Bedeuzzaman, M.V., Farooq, O., Khan, Y.U.: Automatic seizure detection using higher order moments. In: *Proceedings of International Conference on Recent Trends in Information, Telecommunication and Computer* (2010)
14. Guler, I., Ubeyli, E.D.: Multiclass support vector machines for EEG-signals classification. *IEEE Trans. Inf. Technol. Biomed.* **11**(2), 117–126 (2007)
15. Nicolau, N., Georgiou, J.: Detection of epileptic electroencephalogram based on permutation entropy and support vector machine. *Expert Syst. Appl.* **39**, 202–209 (2012)
16. Acharya, U.R., Molinari, F., Sree, S.V., Chattopadhyay, S.: Automatic diagnosis of epileptic EEG using entropies. *Biomed. Signal Process. Control* **7**, 401–408 (2012)
17. Orhan, Umut, Hekim, Mahmut, Ozer, Mahmut: EEG signals classification using the K-means clustering and a multilayer perceptron neural network model. *Expert Syst. Appl.* **38**, 13475–13481 (2011)
18. Das, A.B., Bhuiyan, M.I.H., Alam, S.M.S.: A statistical method for automatic detection of seizure and epilepsy in the dual tree complex wavelet transform domain. In: *IEEE International Conference on Informatics, Electronics and Vision, Bangladesh* (2014)
19. Das, A.B., Bhuiyan, M.I.H., Alam, S.M.S.: Statistical parameters in the dual tree complex wavelet transform domain for the detection of epilepsy and seizure. *IEEE International Conference on Electrical Information and Communication Technology (EICT-2013)*, Bangladesh
20. Chen, G.: Automatic EEG seizure detection using dual-tree complex wavelet-Fourier features. *Expert Syst. Appl.* **41**, 2391–2394 (2014)
21. Mert, A., Akan, A.: Detrended fluctuation thresholding for empirical mode decomposition based denoising. *Digit. Signal Process.* **32**, 48–56 (2014)
22. Selesnick, W., Baraniuk, R.G., Kingsbury, N.: The dual tree complex wavelet transform—a coherent framework for multiscale signal and image processing. *IEEE Signal Process. Mag.* **22**(6), 123–151 (2005)
23. Rahman, S.M.M., Ahmad, M.O., Swamy, M.N.S.: Video denoising based on inter-frame statistical modeling of wavelet coefficients. *IEEE Trans. Circuits Syst. Video Technol.* **17**(2), 187–198 (2007)
24. Li, Y., Li, Y.: Symmetric normal inverse Gaussian and structural similarity based image denoising. In: *Proceedings of multimedia and signal processing. Communications in computer and information science*, vol 346, pp. 103–111. Springer, Heidelberg (2012)
25. Bhuiyan, M.I.H., Ahmad, M.O., Swamy, M.N.S.: Spatially adaptive thresholding in wavelet domain for despeckling of ultrasound images. *IET Image Process.* **03**(03), 147–162 (2009)
26. Bhuiyan, M.I.H., Omair Ahmad, M., Swamy, M.N.S.: Wavelet-based image denoising with the normal inverse Gaussian prior and LMMSE estimator. *IET Image Process.* **02**(4), 203–217 (2008)
27. Hill, P.R., Achim, A.M., Bull, D.R., Al-Mualla, M.E.: Dual-tree complex wavelet coefficient magnitude modelling using the bivariate Cauchy Rayleigh distribution for image denoising. *Signal Process.* **105**, 464–472 (2014)
28. Anantrasirichai, N., Achim, A., Kingsbury, N.G., Bull, D.R.: Atmospheric turbulence mitigation using complex wavelet-based fusion. *IEEE Trans. Image Process.* **22**(6), 2398–2408 (2013)
29. Yang, H., Guan, C., Ang, K.K., Wang, C.C., Phua, K.S., Yu, J.: Dynamic initiation and dual-tree complex wavelet feature-based classification of motor imagery of swallow EEG signals. In: *Proceedings of international joint conference on neural networks (IJCNN)* vol 56, pp. 1–6. IEEE, Brisbane (2012)
30. Bal, U.: Dual tree complex wavelet transform based denoising of optical microscopy images. *Biomed. Opt. Express* **3**(12), 3231–3239 (2012)
31. EEG time series download page. http://epileptologie-bonn.de/cms/front_content.php?idcat=193&lang=3&changelang=3
32. Andrzejak, R.G., Lehnertz, K., Mormann, F., Rieke, C., David, P., Elger, C.E.: Indications of nonlinear deterministic and finite-dimensional structures in time series of brain electrical activity: dependence on recording region and brain state. *Phys. Rev. E Stat. Nonlin. Soft Matter Phys.* **64**, 061907 (2001)
33. Hanssen, A., Oigard, T.A.: The normal inverse Gaussian distribution as a flexible model or heavy-tailed processes. In: *Proceedings of IEEE-EUEASIP Workshop on Non-linear Signals and Image processing* (2001)
34. Andresen, A., Koekebakker, S., Westgaard, S.: Modeling electricity forward prices using the multivariate normal inverse Gaussian distribution. *J. Energy Mark.* **3**(3), 3–25 (2010)
35. Zhang, Xin, Jing, Xili: Image denoising in contourlet domain based on a normal inverse Gaussian prior. *Digit. Signal Process.* **20**, 1436–1439 (2010)
36. Zhou, Y., Wang, J.: Image denoising based on the symmetric normal inverse Gaussian model and non-subsampled contourlet transform. *IET Image Process.* **6**(8), 1136–1147 (2013)
37. Vapnik, V.: An overview of statistical learning theory. *IEEE Trans. Neural Netw.* **10**(5), 988–999 (1999)
38. Dietterich, T.G., Bakiri, G.: Solving multiclass learning problems via error-correcting output codes. *J. Artif. Intell. Res.* **2**, 263–286 (1995)
39. MATLAB. <http://www.mathworks.com/products/matlab/>